THE JOURNAL OF PHYSICAL CHEMISTRY C

Article

pubs.acs.org/JPCC

Molecular and Ionic Dynamics in $Na_xLi_{6-x}C_{60}$

Nicola Sarzi Amadè,[†] Daniele Pontiroli,*[,‡] Luca Maidich,[†] Mauro Riccò,[‡] Mattia Gaboardi,[‡,∥] Giacomo Magnani,[‡] Pietro Carretta,[†] and Samuele Sanna[§]

[†]Dipartimento di Fisica, Università di Pavia, Via Bassi, 6, 27100 Pavia, Italy

[‡]Dipartimento di Scienze Matematiche, Fisiche ed Informatiche, Università di Parma, Viale delle Scienze, 7/a, 43124 Parma, Italy

[§]Department of Physics and Astronomy, University of Bologna, Viale C. Berti Pichat 6/2, 40127 Bologna, Italy

[∥]ISIS Facility, Rutherford Appleton Laboratory, Chilton, Didcot, Oxfordshire OX11 0QX, United Kingdom

ABSTRACT: We report on the C_{60}, Na, and Li dynamics in $Na_xLi_{6-x}C_{60}$ fullerides (x = 0, 1, 5, and 6) in the temperature range 80−550 K by using ^{13}C, ^{23}Na, and ^{7}Li solid state NMR. The results show that the C_{60} reorientation dynamics is hindered at room temperature for the Li-enriched fullerides, but it is active for the Na rich ones with a rate of the order of few kilohertz. ^{23}Na and ^{7}Li NMR measurements show the presence of two dominant thermally activated dynamics that can be associated with Li/Na ionic motions within the octahedral sites (intrasite motion) and between the octahedral and tetrahedral sites (intersite motion). The substitution of one Na or one Li ion in the end members Li_6C_{60} and Na_6C_{60}, respectively, yields to an increase of the hopping rate of the intersite motion, which is necessary for the ionic diffusion in possible fulleride-based ionic conductors.

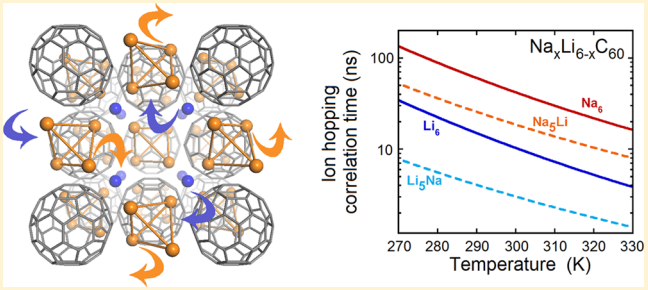

INTRODUCTION

Lithium and sodium cluster-intercalated fullerides (A_xC_{60}; A = Li, Na and x = 6, 12) represent a particular class of alkali fullerides, displaying good performances as hydrogen absorbing materials or as potential components in ion batteries.[1−3] Li and Na ions, thanks to their small ionic radius, are easily intercalated in the interstices of the fullerite lattice with two tetrahedral and one octahedral sites per C_{60} molecule. The crystal structure preserves a face-centered cubic (fcc) symmetry (unlike other A_6C_{60}, A = K, Rb, Cs, which are body-centered cubic), thanks to the formation of small alkali clusters.[4−9]

These clusters seem to play a fundamental role in the hydrogen absorption process, because they allow the H_2 dissociation and the subsequent migration of the H atoms on C_{60} in a reversible way; this mechanism is characterized by significantly faster kinetics and lower hydrogenation temperature than pure C_{60}.[8,10−12] For instance, it has been reported that Li_6C_{60}, $Li_{12}C_{60}$, Na_6C_{60}, and $Na_{10}C_{60}$ can reversibly absorb up to 5, 4.5, 2, and 3.5 wt % H_2 at T = 200−300 °C, respectively,[10,11,13,14] which can be further increased by addition of catalysts such as Pt/Pd nanoparticles.[15] Moreover, these systems also demonstrated to behave as solid absorbers of indirect hydrogen carriers: for example, Li_6C_{60} can reversibly absorb up to 31.2 wt % of ammonia (corresponding to 5.5 wt % hydrogen) at mild conditions.[16] Recently, the combination of Na and Li cointercalated in the $Na_xLi_{6-x}C_{60}$ phases (with x = 0−6) has shown an optimized capacity and kinetics.[17] In particular, $NaLi_5C_{60}$ has proved to absorb up to 4.3 wt % H_2 with an onset temperature 70 °C lower than Li_6C_{60} with the kinetics improved by about 70% and a H_2 desorption enthalpy below 43 kJ/mol H_2.

Furthermore, light alkali and alkali earth (Li, Na, Mg) intercalated fullerides have been received great attention in the recent past, thanks to the ability of the metal ions to diffuse among the C_{60} lattice interstices already at low temperature, thus displaying fast ion conductivity. In particular, Li_4C_{60}, thanks to a peculiar polymeric arrangement of the fullerene units,[18,19] displayed a high Li-ion conductivity of 10^{-2} S/cm at room temperature (a value comparable to that observed in liquid electrolytes) with a relatively low activation energy.[20] Similarly, large Mg-ion conductivity was also observed in the Mg_2C_{60} compound, which is isostructural to Li_4C_{60}.[21] More recently, a detailed NMR and direct current/alternating current (dc/ac) conductivity study on the alkali-cluster intercalated Li_6C_{60} evidenced the presence of room-temperature Li interdiffusive dynamics also in absence of fullerene polymerization, which is hampered upon the hydrogenation of the sample.[22] Some evidence of Na-ions intersite diffusion have been given, either in cubic Na_2C_{60}[23] or in the sodium-cluster intercalated Na_6C_{60},[24] at relatively higher temperature (above T = 400 K). These findings support the possible applications of this class of compounds as solid-state electrolytes in novel ionic batteries.[25−27]

In this work, we report a thorough investigation of selected alkali-cluster intercalated fullerides, $Na_xLi_{6-x}C_{60}$ with x = 0, 1, 5

Received: January 27, 2017
Revised: March 3, 2017
Published: March 6, 2017

DOI: 10.1021/acs.jpcc.7b00887
J. Phys. Chem. C 2017, 121, 6554−6560

and 6, by means of ^{13}C, ^{23}Na, and ^{7}Li solid state NMR in the temperature range 80−550 K in order to investigate the alkali arrangement and the C_{60} and ionic dynamics both in pure and mixed systems. The main result is that the substitution of a single Li(Na) with Na(Li) in the pure Li_6C_{60}(Na_6C_{60}) phase decreases the energy barrier for the ionic diffusion process.

EXPERIMENTAL SECTION

C_{60} powder (99.9% purity) was purchased from MER Corp. The synthesis of the Na and Li cointercalated fullerides is described elsewhere.[17] The X-ray diffraction of these samples shows the formation of single monomeric phases, characterized by an expanded fcc lattice, differently from $Na_xLi_{4-x}C_{60}$ phases that exhibit polymeric structures.[28]

NMR measurements were carried out with a Tecmag Apollo spectrometer at the applied magnetic field of 7 T in the temperature range of 80−550 K. The temperature accuracy is within 1 K. The ^{7}Li and ^{23}Na NMR spectra were obtained from the Fourier transform of half of the echo signal after a solid echo $\pi/2 \rightarrow \tau_{echo} \rightarrow \pi/2$ of radiofrequency (RF) pulse sequence, whereas a standard Hahn echo sequence was used to obtain ^{13}C spectra. The samples (50−80 mg) were sealed in NMR grade quartz vials under 1 mbar He. Saturated solutions of LiCl(aq) (Aldrich, ≥99%) and NaCl(aq) (Aldrich, ≥99%) were used as reference for the shift in the ^{7}Li and ^{23}Na NMR measurements, respectively. ^{13}C-enriched C_{60} (85 wt %) was used as a reference for the ^{13}C NMR measurements.

RESULTS

^{13}C NMR Spectra. Figure 1 shows ^{13}C NMR spectra of $Na_xLi_{6-x}C_{60}$ for x = 0, 1, 5, and 6 in the temperature range

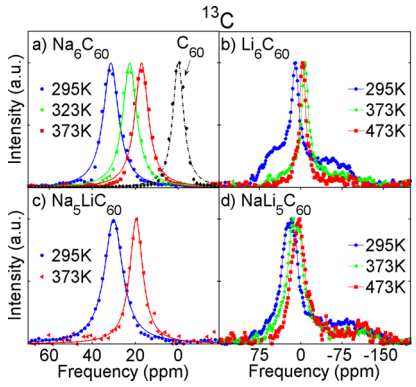

Figure 1. ^{13}C NMR spectra of (a) Na_6C_{60}, (b) Li_6C_{60}, (c) Na_5LiC_{60}, and (d) $NaLi_5C_{60}$ at different temperatures. Frequencies are in ppm with respect to pristine C_{60}, shown in panel (a) for T = 295 K (dashed line). Lines in (a,c) represent the fit to a Lorentzian peak.

295−473 K. The room temperature (RT) spectra of Li_6C_{60} and $NaLi_5C_{60}$ (panels b and d) show a broadened shape characteristic of a chemical-shift-anisotropy (CSA) powder pattern. This structure is typically observed in the static/slow motion regime of pure C_{60} fullerene for T < 140 K.[29] In this regime, for most of the molecules the rate of molecular reorientation is slow compared to the CSA width, $2\pi\Delta\nu_0^{CSA} \approx$ 15 kHz. By increasing the temperature up to 473 K, the spectral lines in Figure 1 b and d get progressively symmetric and narrowed due to thermal activation of large-amplitude molecular reorientation. This behavior is expected when the rate of the C_{60} molecular reorientation becomes larger than $\Delta\nu_0^{CSA}$, driving the system in the fast motion regime.

By contrast, the ^{13}C NMR spectra of Na_6C_{60} and Na_5LiC_{60} (panels a and c) show rather narrow and symmetric lines in the whole temperature range 295−373 K indicating that C_{60} molecular reorientation rate is in the fast motion regime already at RT. By increasing the temperature, a slight decrease of the full width at half-maximum (fwhm) is detected, approaching the value of ∼0.5 kHz at 373 K. This value is the same measured in the fast motion regime at high temperature in pristine C_{60}, (dashed curve in Figure 1a) indicating that for Na_6C_{60} and Na_5LiC_{60} the rotational motion of C_{60} molecules is completely achieved for $T \geq$ 373 K. At 295 K the NMR lines are paramagnetically shifted by about 30 ppm compared to pristine C_{60} in both samples. This value is in agreement with previous NMR and Raman measurements[24,30] that revealed a metallic behavior of this compound in the range 100−300 K. Here the origin of the paramagnetic shift of the ^{13}C signal is related to a non complete charge transfer from the Na to the C_{60} molecule: this generates conductive electrons on the C_{60} molecule that can polarize producing the observed positive shift.[24] By increasing the temperature, this shift gradually decreases for reasons probably due to a temperature-induced charge transfer change, which is now under investigation.

^{7}Li and ^{23}Na NMR Spectra. Panels a and c of Figure 2 show ^{23}Na spectra of Na_6C_{60} and Na_5LiC_{60} measured in the temperature range T = 80−550 K. In both samples, the low-temperature spectrum is characterized by a narrow line at $\nu_1 \sim$ 0 ppm plus a broad one at $\nu_2 \sim$ 130 ppm that can be fit with

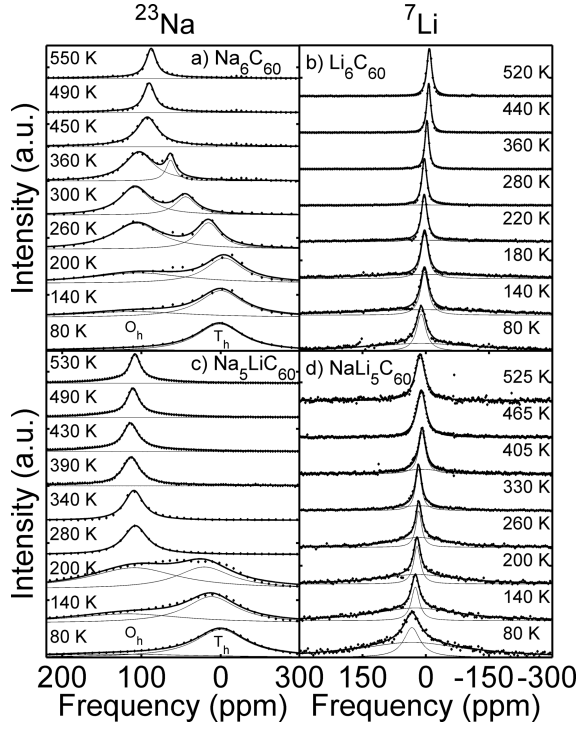

Figure 2. Representative ^{23}Na spectra of (a) Na_6C_{60} and (c) Na_5LiC_{60} for different temperatures. Representative ^{7}Li spectra of (b) Li_6C_{60} and (d) $NaLi_5C_{60}$ for different temperatures. Solid lines are the best fit to a sum of Lorentzian peaks. The zero frequency is referred to ^{7}Li or ^{23}Na resonance in a saturated solution of LiCl(aq) or NaCl(aq), respectively.

DOI: 10.1021/acs.jpcc.7b00887
J. Phys. Chem. C 2017, 121, 6554−6560

Lorentzian curves. The former shows no shift compared to the reference solution, indicating a completely ionized state, whereas the latter is paramagnetically shifted, suggesting the presence of residual charge on Na atoms. By following ref 24, we assign these peaks to Na nuclei belonging to the two chemically inequivalent tetrahedral and octahedral sites of the fcc crystal structure, respectively, at zero and 120 ppm at the lowest T. In fact, the alkali cluster, which is only partially charged, is accommodated in the octahedral void, while the tetrahedral one is not large enough to host more than one ion.[4] For low-temperatures, the octahedral peak gets very broad and is not clearly visible in the spectrum, probably because of a large electric field gradient (EFG) at the Na nuclei generated by the other Na atoms belonging to the same cluster. At high temperatures, the two peaks merge in a single peak as the results of a motional narrowing process[31,32] due to a thermally activated ion dynamics discussed below. Above 400 K, an additional broad line with a width of about 30 kHz is required by the fit in both stoichiometries at the same position of the merged line (this line appears flattened on the scale of panels a and c). This additional line can be attributed to the $\nu_{[\pm 3/2,\pm 1/2]}$ satellite transitions which become evident only when they get narrowed in the fast motion regime.

^{7}Li spectra of Li_6C_{60} and $NaLi_5C_{60}$ are shown in Figure 2b and d, respectively. At low temperature, two lines centered at the same frequency are observed: a narrow peak, which is ascribed to the $\nu_{[1/2,-1/2]}$ central transition, and a broad one, which is ascribed to the $\nu_{[\pm 3/2,\pm 1/2]}$ satellite transitions; these are in agreement with previous measurements.[5,22] The lines associated with the inequivalent tetrahedral and octahedral sites cannot be resolved down to the minimum temperature of 80 K, which is in agreement with recent results that show a moderate line splitting arising only below 70 K.[22]

Figure 3 shows the ^{23}Na spectra for $NaLi_5C_{60}$ and the ^{7}Li spectra for Na_5LiC_{60}. The former exhibits a single line shifted by ∼35 ppm at the lowest temperature investigated (140 K). At 260 K a broader line appears around ∼110 ppm, which gets narrower by increasing the temperature. ^{7}Li spectra in Na_5LiC_{60} show a trend similar to ^{7}Li in $NaLi_5C_{60}$ and Li_6C_{60}: two lines, a narrow one and a broad one, centered at the same frequency are assigned to the central transition and satellite transitions, respectively. Above 400 K, the motional narrowing is reached and there is a single line paramagnetically shifted by ∼50 ppm.

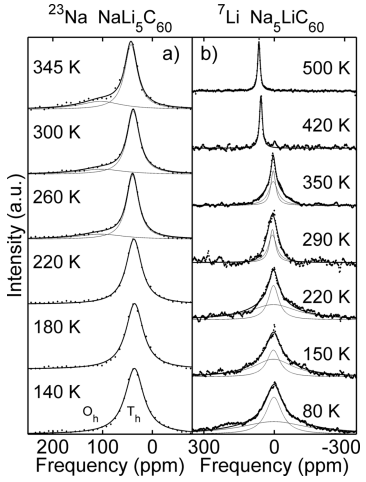

Figure 3. ^{23}Na NMR spectra for $NaLi_5C_{60}$ (left panel) and ^{7}Li NMR spectra for Na_5LiC_{60} (right panel) at different temperatures. Solid lines are the best fit to a sum of Lorentzian peaks. The zero frequency is referred to ^{7}Li or ^{23}Na resonance in a saturated solution of LiCl(aq) or NaCl(aq), respectively.

Spin−Lattice Relaxations of ^{7}Li and ^{23}Na. In order to further study the ionic dynamics, ^{7}Li and ^{23}Na spin−lattice relaxation times, T_1, were measured as a function of temperature using a standard saturation recovery pulse sequence. For all the T_1 measurements, the recovery of the nuclear magnetization as a function of the delay between the saturating and the readout pulses (not shown) can be properly fit by the standard recovery law

$$M(t) = M_\infty\left[1 - \exp\left(-\frac{t}{T_1}\right)^{\beta}\right] \quad (1)$$

suggesting that a large portion of the satellite is being irradiated. The stretching exponent β increases from ∼0.6 to 1 by increasing the temperature from 80 to 400 K. Figure 4 shows

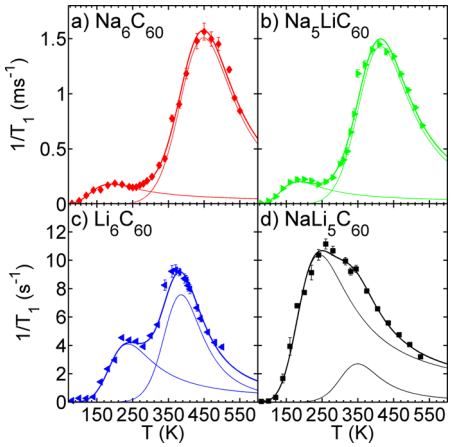

Figure 4. Temperature evolution of the inverse spin−lattice relaxation time, $T_1^{-1}(T)$, of ^{23}Na for (a) Na_6C_{60}, (b) Na_5LiC_{60}, and of ^{7}Li for (c) Li_6C_{60} and (d) $NaLi_5C_{60}$. Solid lines are the results of the fit to a sum of two BPP-type functions (see text).

the temperature evolution of $1/T_1$ of ^{7}Li for Li_6C_{60} and $NaLi_5C_{60}$ and of ^{23}Na for Na_6C_{60} and Na_5LiC_{60}. All the plots display the same qualitative behavior with two peaks of the $1/T_1(T)$. The best curve fits (solid lines) are always obtained by a sum of two BPP functions[33]

$$\frac{1}{T_1} \approx \sum_{i=1,2} \frac{D_i\tau_{c,i}}{1+\omega_L^2\tau_{c,i}^2} + \frac{4D_i\tau_{c,i}}{1+4\omega_L^2\tau_{c,i}^2} \quad (2)$$

which consider fluctuations described by two different thermally activated correlation times

$$\tau_{c,i} = \tau_{\infty,i}\exp\left(\frac{E_{a,i}}{k_B T}\right)(i = 1, 2) \quad (3)$$

D_i is a constant, $E_{a,i}$ is the activation energy associated with the process and ω_L is the ^{23}Na or ^{7}Li Larmor frequency. The fit outcomes for $E_{a,i}$ and $\tau_{\infty,i}$ are shown in Table 1.

The ^{23}Na and ^{7}Li spin−lattice relaxation times are of the order of 1 and 100 ms respectively, that is, the ratio is $R = T_{1,Na}^{-1}/T_{1,Li}^{-1} \sim 10^2$. If dipolar magnetism dominated the fluctuation mechanism, R would be likely of the order of the ratio between the square of the gyromagnetic ratio, $\gamma_{Na}^2/\gamma_{Li}^2 \approx 4$,

DOI: 10.1021/acs.jpcc.7b00887
J. Phys. Chem. C 2017, 121, 6554−6560

Table 1. Comparison of Activation Energies (in meV Units) and Correlation Times (in ps Units) Obtained in This Work from T_1 Spin−Lattice Relaxation Measurements

sample	nucleus	$E_{a,1}$	$\tau_{\infty,1}$	$E_{a,2}$	$\tau_{\infty,2}$
Li_6C_{60}	^{7}Li	88(5)	12(1)	280(10)	0.2(0.1)
$NaLi_5C_{60}$	^{7}Li	78(5)	21(3)	220(20)	0.6(0.2)
Na_5LiC_{60}	^{23}Na	53(5)	45(4)	240(10)	1.7(0.1)
Na_6C_{60}	^{23}Na	48(5)	64(20)	270(10)	1.2(0.1)

in contrast with the experimental behavior. Instead, the electric field gradient fluctuations at the nuclei give rise to a relaxation rate proportional to the square of the quadrupole frequency, ν_Q. It is possible to roughly consider $\nu_Q \propto QV_0(1-\gamma_\infty)$, being Q the quadrupole moment, V_0 is the electric field gradient due to the changes surrounding the nuclei, and γ_∞ is the Sternheimer antishielding factor. Considering that $(1-\gamma_\infty^{Na+})/(1-\gamma_\infty^{Li+}) \approx 4$ and that $Q_{Na}/Q_{Li} \approx 2.7$ and by assuming that V_0 is roughly constant (that is, that the charge distribution around the Na and Li nuclei is similar), one finds that $\nu_{Q,Na}^2/\nu_{Q,Li}^2 \approx 110$, which is in reasonable agreement with the experimental value of R. This suggests that the relaxation mechanism of $Na_xLi_{6-x}C_{60}$ is dominated by the fluctuation of the quadrupolar coupling, making the $1/T_1(T)$ behavior an excellent probe of the ion dynamics trough the fluctuations of the electric field gradient around the ^{23}Na or ^{7}Li nuclei, for example, due to the ionic motion.

DISCUSSION

The results allow us to investigate the molecular and ionic dynamics of $Na_xLi_{6-x}C_{60}$. In the following, we discuss the C_{60} molecular reorientation dynamics first and the ionic dynamics afterward. The ^{13}C NMR spectra in Figure 1 show that the C_{60} molecular reorientation rate is in the fast motion regime (well above tens of kilohertz) already at RT both in Na_6C_{60} and Na_5LiC_{60}, as discussed in ^{13}C NMR Spectra. On the contrary, for the Li_6C_{60} and $NaLi_5C_{60}$ compounds the molecular reorientation is partially frozen out at RT and temperatures above 350 K are needed to activate all the rotational motions. Actually, Li_6C_{60} has a considerably smaller lattice constant than Na_6C_{60} (at room temperature 13.815 and 14.380 Å, respectively[4,12]), for steric reasons, since Na ion is larger than Li ion. In addition, there is a possible hybridization of the C_{60} LUMO with the Li atomic orbitals.[34] For these reasons, lithium, rather than Na, is more likely to hinder the C_{60} rotations. By assuming that the crystal structure does not change significantly by substituting a Li atom with a Na one (and vice versa), the same argument can be extended to $NaLi_5C_{60}$ and Na_5LiC_{60}, which at room temperature are in the slow and fast motional regime, respectively, similarly to their respective pure Li and Na counterpart.

Concerning the Li^+ and Na^+ ionic motion, the results reveal for all samples the presence of two different processes in the temperature range here explored. These are evidenced by the two peaks observed in the $1/T_1(T)$ behavior displayed in Figure 4. This behavior has been successfully fitted by using two BPP functions as explained in Spin−Lattice Relaxations of ^{7}Li and ^{23}Na. The BPP peak is expected for $\omega_L\tau_c = 1$, that is, when the frequency of the fluctuations, $1/\tau_c$, matches the Larmor frequency. Because in our experimental conditions the Larmor frequency was $\omega_L^{Li} \approx 700$ rad/s and $\omega_L^{Na} \approx 500$ rad/s for Li and Na, respectively, the two dynamics have correlation times of the order of few nanoseconds at the peak temperature, occurring in two distinct temperature range of ∼150−200 and ∼300−450 K. The correlation times in the limit of high temperature (τ_∞) and the activation energies (E_a) of the two dynamics, evaluated from eq 2, are summarized in Table 1.

The same dynamics also induces the narrowing of the NMR line width when the correlation time is of the order of the inverse of the line width measured at low temperature, that is, in the static regime, which in our case is of the order of $\tau_c \approx 1/(2\pi\Delta\nu_0) \sim 10^{-5}-10^{-4}$ s. This is a much larger time scale than that probed by the $1/T_1$ discussed above, which means that the narrowing effect is shifted to lower temperatures with respect to the $1/T_1$ peak for each dynamics. By considering the activation energies $E_{a,1} \sim 60$ meV and $E_{a,2} \sim 250$ meV and $\tau_{\infty,1} \sim 30$ ps and $\tau_{\infty,2} \sim 1$ ps (Table 1) for the two dynamics, from eq 3 we can roughly estimate that a narrowing of the line width should occur above $T \sim 30-40$ K and above $T \sim 140-160$ K, respectively. The latter value is fully consistent with the line narrowing process occurring above 150−200 K, as shown in both Figures 5 and 6. The narrowing expected at $T \sim 30-40$ K is well below the temperature range that we have explored here and we have no clear evidence of that. Nevertheless, a fast decrease of the line width is observed around 80 K in both Na_6C_{60} and Na_5LiC_{60} in Figure 5 for the octahedral peak, which could be the tail of this low temperature dynamics.

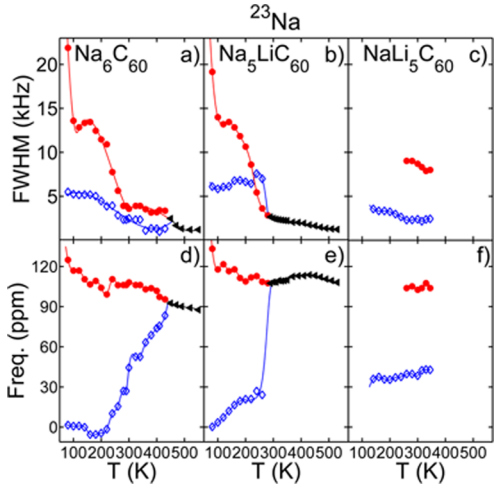

Figure 5. fwhm and frequency temperature dependence of ^{23}Na NMR spectra for Na_6C_{60}, Na_5LiC_{60}, and $NaLi_5C_{60}$, for octahedral (full symbols) and tetrahedral (open symbols) sites. At high temperatures, the octahedral and tetrahedral signals merge (triangles) for Na_6C_{60}, Na_5LiC_{60}. The solid lines are guides to the eye.

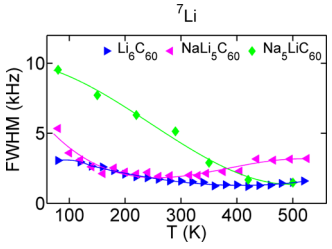

Figure 6. fwhm temperature dependence of ^{7}Li spectra for Li_6C_{60}, $NaLi_5C_{60}$, and Na_5LiC_{60}. The solid lines are guides to the eye.

In order to understand what kind of dynamical process is responsible for the observed behavior, we can consider the evolution of the position of the ^{23}Na NMR peaks in the

DOI: 10.1021/acs.jpcc.7b00887
J. Phys. Chem. C 2017, 121, 6554−6560

octahedral and tetrahedral sites of Na_6C_{60}, displayed in Figure 5d. Here a gradual narrowing and a progressive shift of both peaks occurs above $T \simeq 200$ K and the two frequencies eventually merge above 400 K. The merging of the two lines can be attributed to the Na ions hopping motion between the octahedral and tetrahedral sites, which is in agreement with previous results.[24] This motion averages the two inequivalent positions when the jump rate exceeds the difference between their peak frequency $2\pi\Delta \sim 50$ kHz. Therefore, we can label this process as intersite motion.

The phenomenology of Na_5LiC_{60} (Figure 5e) is very similar to the previous case but here the two peaks merge (abruptly) at a lower temperature. This is remarkable behavior because it indicates that the effect of the substitution of one Na with one Li atom in Na_6C_{60} increases the overall Na interstite mobility. This is also in agreement with a reduced value of the activation energy for the intersite motion, E_2, of this compound with respect to that of pure Na_6C_{60}, as reported in Table 1.

On the contrary, the behavior of Na ion in $NaLi_5C_{60}$ is significantly different. For this sample, we can distinguish the two peaks associated with Na in the octahedral and tetrahedral sites also well above the room temperature with their resonance frequency almost unchanged, as shown in Figure 5f. This behavior suggests that the intersite motion of the Na ions is hindered here, most likely because of the narrowing of the channels connecting the tetrahedral and octahedral sites owing to the volume shrinkage caused by the smaller Li ions steric hindrance, as compared with Na_6C_{60}. This seems to be sufficient to suppress the intersite motion of the Na ions in $NaLi_5C_{60}$, but not the motion of the smaller Li ones.

The intersite motion of the smaller Li^+ is revealed by the high temperature peak in the $1/T_1(T)$ curves in Figure 4c,d, as well as by the progressive reduction of the ^{7}Li NMR line width already above 100 K in Figure 6 for Li_6C_{60}, $NaLi_5C_{60}$, and Na_5LiC_{60}, which is in agreement with the results previously reported for Li_6C_{60}.[22] Incidentally, at high temperature in Figure 6 we also observe a moderate increase of the line width of Li_6C_{60} and $NaLi_5C_{60}$ above 400 K, possibly due to a structural transition.

Figure 7 shows the trend of correlation times for the intersite dynamics, $\tau_{c,2}$, for all the investigated $Na_xLi_{6-x}C_{60}$ compounds, as calculated from eq 3 and data in Table 1, around room temperature. The data show that there is a reduction of $\tau_{c,2}$, that is, an increase of the hopping rate of the intersite motion, when one Li is substituted by one Na in Li_6C_{60}, as well as when one Na is substituted by one Li in the Na_6C_{60} counterpart. This is a remarkable result, because the intersite hopping process sustains the Li^+ and Na^+ long-range diffusion dynamics, which is necessary for possible application of this class of compounds as solid-state electrolytes in novel ionic batteries. In particular, the correlation time of these dynamics at room temperature is found to be of the order of 1−100 ns. If one considers a simple hopping model based on the Nerst−Einstein equation,[22,35] this value appears compatible with a sizable ionic diffusion current in these systems, hence useful for applications. In fact, previous ac/dc conductivity measurements[22] performed on Li_6C_{60} have shown that this system behaves as an ionic conductor with a room temperature conductivity of the order of 10^{-5} S cm^{-1}. The results in Figure 7 suggest that the ionic conductivity might be further enhanced in Li_6C_{60} when one Li is substituted by a Na atom and, similarly, it could be improved in Na_6C_{60} by substituting one Na by Li. ac/dc conductivity measurements are needed to further investigate this fulleride family and to provide a direct measurement of the ionic Li and Na diffusivity.

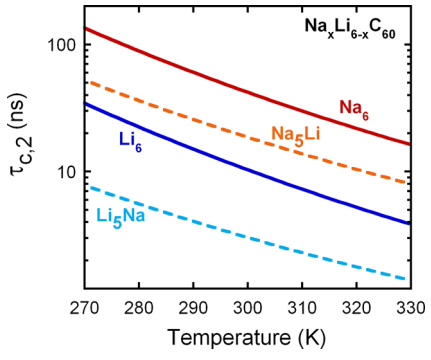

Figure 7. Correlation times of the intersite hopping motion, $\tau_{c,2}$, of the predominant alkali species for $Na_xLi_{6-x}C_{60}$ (x = 0, 1, 5, 6) around room temperature, calculated by using eq 3 and data in Table 1.

Above, we have seen that the resonance line positions of the intercalated alkali metals are mainly indicative of the occupied interstice (either octahedral or tetrahedral). By assuming a paramagnetic shift as an indication of electron density located around the nucleus, the positive shift observed for the octahedral ions, that is, those forming the clusters, indicates a partial ionization of these ions, implying a reduced transfer of electrons to C_{60} with respect to the six expected. This effect, already reported in other studies,[5] is important for the application of these materials as hydrogen absorbers. During the first stage of the chemical absorption process, the hydrogen molecules get dissociated into two hydrogen atoms. This process, known as hydrogen spillover effect,[36] is mediated by metallic clusters (alkali clusters in our case).[37] The efficiency of the intercalated clusters to induce the H_2 dissociation is then related to the amount of electron density localized within the cluster, that is, to the metallic character of the constituent ions, which can be probed by measuring the NMR shift. From the position of the ^{13}C resonance lines shown in Figure 1, a temperature-induced diamagnetic shift is observed as a general trend for all the samples. This is an indication that on increasing the temperature, some electron density is back-donated to the alkali ions, in particular to the octahedral clusters. In fact, the opposite trend is observed in Figures 2a,c and 3b in which an overall paramagnetic shift is shown, mainly due to the temperature activated migration of the tetrahedral ions into the octahedral clusters. These results then suggest that the relatively high temperatures required to induce the hydrogen absorption in these C_{60} based systems, as mentioned in the introduction paragraph, may be due to the insufficient electron density on the octahedral cluster present at lower temperatures. This important hint needs however to be confirmed by further investigations.

CONCLUSIONS

Summarizing, we have studied the C_{60} molecular and Na/Li ionic dynamics in $Na_xLi_{6-x}C_{60}$ fullerides with x = 0, 1, 5, and 6 exploiting the ^{13}C, ^{7}Li and ^{23}Na NMR probes. ^{13}C NMR evidence a thermally activated reorientation of C_{60}, which is promoted above the rate of few kilohertz at temperatures well below(above) RT for fullerides with Na(Li) as a major dopant. A thermally induced back-donation of electron density to the alkali ions is also suggested by the ^{13}C NMR shift. The analysis of the relaxation rate $1/T_1$ and of the NMR spectra of ^{7}Li/^{23}Na

DOI: 10.1021/acs.jpcc.7b00887
J. Phys. Chem. C 2017, 121, 6554−6560

NMR measurements clearly indicates two ionic dynamics with distinct activation energies E_a, summarized in Table 1: an intrasite dynamics, that is, a local motion within the octahedral sites with $E_{a,1} \approx 50-90$ meV, and an intersite motion between the octahedral and tetrahedral sites with $E_{a,2} \approx 220-280$ meV. The substitution of one Na or one Li ion in the end members Li_6C_{60} and Na_6C_{60}, yields to an increase of the hopping rate for the intersite motion of Li and Na, respectively, responsible for the effective ionic conductivity of the alkali ion. The results of this work stimulate for a direct measurement of the ionic conductivity in fullerides with Li/Na mixture. Furthermore, the comprehension of the Na and Li processes above room temperature can be important to further understand the hydrogenation activation mechanism.

AUTHOR INFORMATION

Corresponding Author

*E-mail: daniele.pontiroli@fis.unipr.it. Phone: +39 0521 905236. Fax: +39 0521 905223.

ORCID

Nicola Sarzi Amadè: 0000-0001-6932-7827

Mauro Riccò: 0000-0002-6879-2687

Mattia Gaboardi: 0000-0003-3340-4469

Notes

The authors declare no competing financial interest.

ACKNOWLEDGMENTS

The authors thank C. Milanese for useful discussions. The authors gratefully acknowledge Fondazione CARIPLO for fundings (Project number 2013-0592). M.G. acknowledges the European Union's Horizon 2020 research and innovation programme under the Marie Sklodowska-Curie Grant Agreement 665593 awarded to the Science and Technology Facilities Council.

REFERENCES

(1) Jena, P. Materials for Hydrogen Storage: Past, Present, and Future. *J. Phys. Chem. Lett.* **2011**, *2*, 206−211.

(2) Loutfy, R. O.; Katagiri, S. In *Perspectives of Fullerene Nanotechnology*; Osawa, E., Ed.; Springer Netherlands: Dordrecht, 2002; pp 357−367.

(3) Zhang, R. G.; Mizuno, F.; Ling, C. Fullerenes: Non-Transition Metal Clusters as Rechargeable Magnesium Battery Cathodes. *Chem. Commun. (Cambridge, U. K.)* **2015**, *51*, 1108−1111.

(4) Rosseinsky, M. J.; Murphy, D. W.; Fleming, R. M.; Tycko, R.; Ramirez, A. P.; Siegrist, T.; Dabbagh, G.; Barrett, S. E. Structural and Electronic Properties of Sodium-Intercalated C60. *Nature* **1992**, *356*, 416−418.

(5) Tomaselli, M.; Meier, B. H.; Riccò, M.; Shiroka, T.; Sartori, A. A Multiple-Quantum Nuclear Magnetic Resonance Study of Interstitial Li Clusters in LixC60. *J. Chem. Phys.* **2001**, *115*, 472−476.

(6) Cristofolini, L.; Riccò, M.; De Renzi, R. NMR and High-Resolution X-ray Diffraction Evidence for an Alkali-Metal Fulleride with Large Interstitial Clusters: Li12C60. *Phys. Rev. B: Condens. Matter Mater. Phys.* **1999**, *59*, 8343−8346.

(7) Gaboardi, M.; Cavallari, C.; Magnani, G.; Pontiroli, D.; Rols, S.; Riccò, M. Hydrogen Storage Mechanism and Lithium Dynamics in Li12C60 Investigated by μSR. *Carbon* **2015**, *90*, 130−137.

(8) Mauron, P.; Remhof, A.; Bliersbach, A.; Borgschulte, A.; Züttel, A.; Sheptyakov, D.; Gaboardi, M.; Choucair, M.; Pontiroli, D.; Aramini, M.; et al. Reversible Hydrogen Absorption in Sodium Intercalated Fullerenes. *Int. J. Hydrogen Energy* **2012**, *37*, 14307−14314.

(9) Yildirim, T.; Zhou, O.; Fischer, J. E.; Bykovetz, N.; Strongin, R. A.; Cichy, M. A.; Smith, A. B., III; Lin, C. L.; Jelinek, R. Intercalation of Sodium Hetero-Clusters into the C60 Lattice. *Nature* **1992**, *360*, 568−571.

(10) Teprovich, J. A.; Wellons, M. S.; Lascola, R.; Hwang, S.-j.; Ward, P. A.; Compton, R. N.; Zidan, R. Synthesis and Characterization of a Lithium-Doped Fullerane (Lix-C60- Hy) for Reversible Hydrogen Storage. *Nano Lett.* **2012**, *12*, 582−589.

(11) Mauron, P.; Gaboardi, M.; Pontiroli, D.; Remhof, A.; Riccò, M.; Züttel, A. Hydrogen Desorption Kinetics in Metal Intercalated Fullerides. *J. Phys. Chem. C* **2015**, *119*, 1714−1719.

(12) Gaboardi, M.; Duyker, S.; Milanese, C.; Magnani, G.; Peterson, V. K.; Pontiroli, D.; Sharma, N.; Riccò, M. In Situ Neutron Powder Diffraction of Li6C60 for Hydrogen Storage. *J. Phys. Chem. C* **2015**, *119*, 19715−19721.

(13) Teprovich, J. A.; Knight, D. A.; Peters, B.; Zidan, R. Comparative Study of Reversible Hydrogen Storage in Alkali-Doped Fulleranes. *J. Alloys Compd.* **2013**, *580*, S364−S367.

(14) Mauron, P.; Gaboardi, M.; Remhof, A.; Bliersbach, A.; Sheptyakov, D.; Aramini, M.; Vlahopoulou, G.; Giglio, F.; Pontiroli, D.; Riccò, M.; et al. Hydrogen Sorption in Li12C60. *J. Phys. Chem. C* **2013**, *117*, 22598−22602.

(15) Aramini, M.; Milanese, C.; Pontiroli, D.; Gaboardi, M.; Girella, A.; Bertoni, G.; Riccò, M. Addition of Transition Metals to Lithium Intercalated Fullerides Enhances Hydrogen Storage Properties. *Int. J. Hydrogen Energy* **2014**, *39*, 2124−2131.

(16) Pontiroli, D.; D'Alessio, D.; Gaboardi, M.; Magnani, G.; Milanese, C.; Duyker, S. G.; Peterson, V. K.; Sharma, N.; Riccò, M. Ammonia-Storage in Lithium Intercalated Fullerides. *J. Mater. Chem. A* **2015**, *3*, 21099−21105.

(17) Gaboardi, M.; Milanese, C.; Magnani, G.; Girella, A.; Pontiroli, D.; Ricco, M. Sodium Catalytic Effect in the $Na_xLi6_{-x}C60$ Hydrogen Storage Process. ArXiv e-prints 2016, arXiv:1611.06512, arXiv.org e-Print archive, http://arxiv.org/abs/1611.06512 (accessed Nov 20, 2016).

(18) Riccò, M.; Shiroka, T.; Belli, M.; Pontiroli, D.; Pagliari, M.; Ruani, G.; Palles, D.; Margadonna, S.; Tomaselli, M. Unusual Polymerization in the Li4C60 Fulleride. *Phys. Rev. B: Condens. Matter Mater. Phys.* **2005**, *72*, 1−7.

(19) Rols, S.; Pontiroli, D.; Cavallari, C.; Gaboardi, M.; Aramini, M.; Richard, D.; Johnson, M. R.; Zanotti, J. M.; Suard, E.; Maccarini, M.; et al. Structure and Dynamics of the Fullerene Polymer Li4C60 Studied with Neutron Scattering. *Phys. Rev. B: Condens. Matter Mater. Phys.* **2015**, *92*, 014305.

(20) Riccò, M.; Belli, M.; Mazzani, M.; Pontiroli, D.; Quintavalle, D.; Jánossy, A.; Csányi, G. Superionic Conductivity in the Li4C60 Fulleride Polymer. *Phys. Rev. Lett.* **2009**, *102*, 2−5.

(21) Pontiroli, D.; Aramini, M.; Gaboardi, M.; Mazzani, M.; Gorreri, A.; Riccò, M.; Margiolaki, I.; Sheptyakov, D. Ionic Conductivity in the Mg Intercalated Fullerene Polymer Mg2C60. *Carbon* **2013**, *51*, 143−147.

(22) Maidich, L.; Pontiroli, D.; Gaboardi, M.; Lenti, S.; Magnani, G.; Riva, G.; Carretta, P.; Milanese, C.; Marini, A.; Riccò, M.; et al. Investigation of Li and H Dynamics in Li6C60 and Li6C60Hy. *Carbon* **2016**, *96*, 276−284.

(23) Klupp, G.; Matus, P.; Quintavalle, D.; Kiss, L.; Kováts, É; Nemes, N.; Kamarás, K.; Pekker, S.; Jánossy, a. Phase Segregation on the Nanoscale in Na2C60. *Phys. Rev. B: Condens. Matter Mater. Phys.* **2006**, *74*, 195402.

(24) Rachdi, F.; Hajji, L.; Galtier, M.; Yildirim, T.; Fischer, J. E.; Goze, C.; Mehring, M. 13C and 23Na NMR Studies of Na2C60 and Na6C60 Fullerides. *Phys. Rev. B: Condens. Matter Mater. Phys.* **1997**, *56*, 7831−7834.

(25) Cattaneo, A. S.; Dall'Asta, V.; Pontiroli, D.; Riccò, M.; Magnani, G.; Milanese, C.; Tealdi, C.; Quartarone, E.; Mustarelli, P. Tailoring Ionic-Electronic Transport in PEO-Li4C60: Towards a New Class of All Solid-State Mixed Conductors. *Carbon* **2016**, *100*, 196−200.

DOI: 10.1021/acs.jpcc.7b00887
J. Phys. Chem. C 2017, 121, 6554−6560

(26) Zhang, R.; Mizuno, F. Fullerenes as High Capacity Cathode Materials for a Rechargeable Magnesium Battery.2015; Patent App. US14/045,906.
(27) Zhang, R.; Mizuno, F. Fullerene Cathodes for a Rechargeable Magnesium Battery. 2015; Patent App. WOPCT/US2014/055.
(28) Röding, R.; Wågberg, T.; Sundqvist, B. Structural Properties of the Polymeric Compounds LixNa(4-x)C60. *Chem. Phys. Lett.* **2005**, *413*, 157−161.
(29) Tycko, R.; Dabbagh, G.; Rosseinsky, M. J.; Murphy, D. W.; Fleming, R. M.; Ramirez, A. P.; Tully, J. C. 13C NMR Spectroscopy of KxC60: Phase Separation, Molecular Dynamics, and Metallic Properties. *Science* **1991**, *253*, 884−886.
(30) Duclos, S. J.; Haddon, R. C.; Glarum, S.; Hebard, A. F.; Lyons, K. B. Raman Studies of Alkali-Metal Doped AxC60 Films (A = Na, K, Rb, and Cs; x = 0. 3, and 6). *Science* **1991**, *254*, 1625−1627.
(31) Abragam, A. *Principles of Nuclear Magnetism*; Oxford University Press: Oxford, U.K, 1963.
(32) Pontiroli, D.; Aramini, M.; Gaboardi, M.; Mazzani, M.; Sanna, S.; Caracciolo, F.; Carretta, P.; Cavallari, C.; Rols, S.; Tatti, R.; et al. Tracking the Hydrogen Motion in Defective Graphene. *J. Phys. Chem. C* **2014**, *118*, 7110−7116.
(33) Bloembergen, N.; Purcell, E.; Pound, R. Relaxation Effects in Nuclear Magnetic Resonance Absorption. *Phys. Rev.* **1948**, *73*, 679−715.
(34) Hirosawa, I.; Prassides, K.; Mizuki, J.; Tanigaki, K.; Gevaert, M.; Lappas, A.; Cockcroft, J. K. Orientational Disorder of C60 in Li2CsC60. *Science* **1994**, *264*, 1294−1297.
(35) Matsuo, M.; Nakamori, Y.; Orimo, S.; Maekawa, H.; Takamura, H. Lithium Superionic Conduction in Lithium Borohydride Accompanied by Structural Transition. *Appl. Phys. Lett.* **2007**, *91*, 224103.
(36) Curtis Conner, W.; Pajonk, G. M.; Teichner, S. J. Spillover of Sorbed Species. *Adv. Catal.* **1986**, *34*, 1−79.
(37) Aramini, M.; Gaboardi, M.; Vlahopoulou, G.; Pontiroli, D.; Cavallari, C.; Milanese, C.; Riccò, M. Muon Spin Relaxation Reveals the Hydrogen Storage Mechanism in Light Alkali Metal Fullerides. *Carbon* **2014**, *67*, 92−97.

DOI: 10.1021/acs.jpcc.7b00887
J. Phys. Chem. C 2017, 121, 6554−6560